Electronic Supporting Information for

First Cu-Nanostar as Sustainable Catalyst Realized through Synergistic Effects of Bowl-shaped Features and Surface Activation of Sporopollenin Exine

Vijayendran Gowri,[a,b,†] Sarita Kumari,[a,†] Raina Sharma,[a] Abdul Selim,[a] Govindasamy Jayamurugan [a,*]

[a]Institute of Nano Science and Technology, Knowledge City, Sector 81, Mohali, Punjab 140306, India

[b]Gowriz Skincare Pvt Ltd incubated at Technology Business Incubator (TBI) at IISER Mohali, Knowledge City, Sector 81, Mohali, Punjab 140306, India

Correspondence to Govindasamy Jayamurugan (E-mail: jayamurugan@inst.ac.in; jayamuruganinst@gmail.com)

Table of Contents

Section A: (i) General Information

Lycopodium powder (Microtroniks Quali-tech Chem) was purchased from amazon (India) Pvt Ltd. The deionized water (DI-H_2O) was obtained using the Merck-Millipore water purifier system. $CuCl_2$ was purchased from Loba Chemie. All the reagents were purchased commercially (Tokyo Chemical Industry (India) Pvt. Ltd. and Sigma Aldrich) including polyethyleneimine (PEI, Mw ~750,000 Daltons by LS, 50 wt% in H_2O, Sigma Aldrich) and used without any further purification.

(ii) Instrumentation

Attenuated total reflection Fourier transform infrared (ATR-FT-IR) spectroscopy Transmission spectra were measured using an Agilent Cary 660 spectrometer in the range of 4000−500 cm^{-1}.

Powder X-ray diffraction (PXRD) was performed using a Bruker D-8 advanced diffractometer inthe 2θ range of 30–80°.

^{1}H- and ^{13}C-nuclear magnetic resonance (NMR) spectra were measured on a Bruker Advance-II spectrometer at 400 MHz and 100 MHz, respectively, using DMSO-d_6 or $CDCl_3$ as solvent. The chemical shift was reported in parts per million (ppm) relative to tetramethylsilane (TMS) as the internal standard. Data for ^{1}H-NMR and ^{13}C-NMR are reported as follows: s = singlet, d = doublet, t = triplet, dd = doublet of doublets, m = multiplet.

X-ray photoelectron spectroscopy (XPS) spectra were recorded using a PHI 5000 Versa Probe high-performance electron spectrometer, coupled with monochromatic Al-Kα radiation (1486.6 eV) operating at an accelerating X-ray power of 50 W and 15 kV. The sample was outgassed at 25 °C in a UHV chamber (<5 × 10^{-7} Pa) before the measurement.

Inductively coupled plasma-mass spectrometer (ICP-MS) was used to estimate the amount of copper in the catalyst using ICP-MS, Agilent Technologies 7700 series. Then, 2 mg of sample in 10 mL of aqua regia were digested in the microwave for 2 h at 185 °C. The resulting solution was diluted and analyzed using ICP-MS.

Transmission electron microscopy (TEM) images and elemental mapping were acquired on a Jeol TEM 2100 Plus operating at 120 kV. Samples were prepared by depositing a drop of diluted nanoparticle solution on a 300 mesh TEM gold grid and dried under vacuum for 24 h.

Gas chromatography-mass spectrometry (GC-MS) analysis was performed using an Agilent GC-MS (5977C) with triple Axis Detector with long life triple channel EM mass detector with (5%-phenyl)-methylpolysiloxane nonpolar column. GC-MS operating conditions: The initial oven

temperature was 50 °C, maintained for 1 min and then ramped to 270 °C at a rate of 5 °C/min followed by holding for 3 min at 270 °C. The initial temperature of the injector was 50 °C and then programmed at the same rate as the oven. Helium was used as a carrier gas with primary pressure of 570 KPa. The split injection mode was used with a split ratio of 10.0. The injection volume of each sample was 1 µL. Mass spectrometer settings: electron impact ionization mode with electron energy of 70 eV, ion source was set at 270 °C and scan mass range *m/z* 50–550.

Thermogravimetric analysis (TGA) was performed using a thermogravimetric analyzer (Perkin Elmer STA 8000) at an N_2 flow rate of 10 mL/min and a heating rate of 10 °C/min.

The diffuse ultraviolet-visible reflectance spectra were measured using a Shimadzu UV/Vis spectrophotometer (UV 2600) with $BaSO_4$ as an internal standard.

Section B: Experimental Section

Synthetic procedures for catalyst ESP-PEI-$Cu^{I/II}$O-NS

To obtain large and uniform cavity spore precursor which is free of other genetic materials for the synthesis of ESP-PEI-$Cu^{I/II}$O-NS nanostars, raw lycopodium clavatum sporopollenin powder, by following the reported procedure.[S1] Briefly, the synthesis of ESP-PEI-$Cu^{I/II}$O-NS was achieved by three-step processes.

i) Raw spores (100 g) were refluxed in acetone (500 mL) for 4 h, filtered and dried to yield deflated spores. After refluxing in 6% KOH solution (500 mL) for 6 h, it was filtered and the process was repeated once more. The spores were washed with hot water (2 × 50 mL), hot ethanol (300 mL), and dried on an open air (15 h). Afterwards, it was suspended in 75% H_3PO_4 (500 mL) and refluxed for 7 days, filtered, washed with water (3 × 600 mL), acetone (500 mL), 2M HCl (600 mL), 2M NaOH (600 mL), once again with water (5 × 500 mL) and acetone (600 mL) successively, and dried in open air to obtain ESP (80 g) as colourless powder.

ii) The exine capsules (100 mg) were functionalized with PEI (50 mg) in DMF (10 mL) at 50 °C for 24 h using passive encapsulation technique. The solution was centrifuged and was successively with 3×100 mL H_2O and 3×100 mL EtOH and dried overnight in vacuum oven at 50 °C, and was named as ESP-PEI (100 mg) as faint yellow coloured solid.

iii) Treatment of PEI functionalized sporopollenin (ESP-PEI, 50 mg) with $CuCl_2$ (100 mg) in EtOH/H_2O 1:1 medium for 2 h and then was centrifuged and washed with 3 × 5 mL EtOH to generate $Cu^{I/II}$O nanostar (ESP-PEI-$Cu^{I/II}$O-NS) which was then vacuum oven dried at 50 °C for overnight to obtain 40 mg of faint green colored solid.

Section C: Characterization of ESP-PEI-Cu$^{I/II}$O-NS.

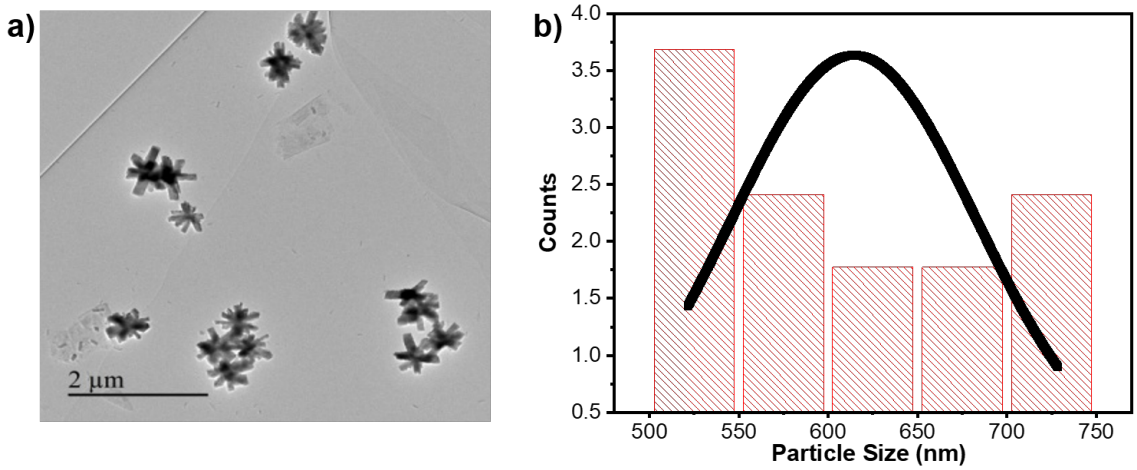

Fig. S1 (a) TEM of ESP-PEI-Cu$^{I/II}$O-NS (b) Size distribution curve for ESP-PEI-Cu$^{I/II}$O-NS.

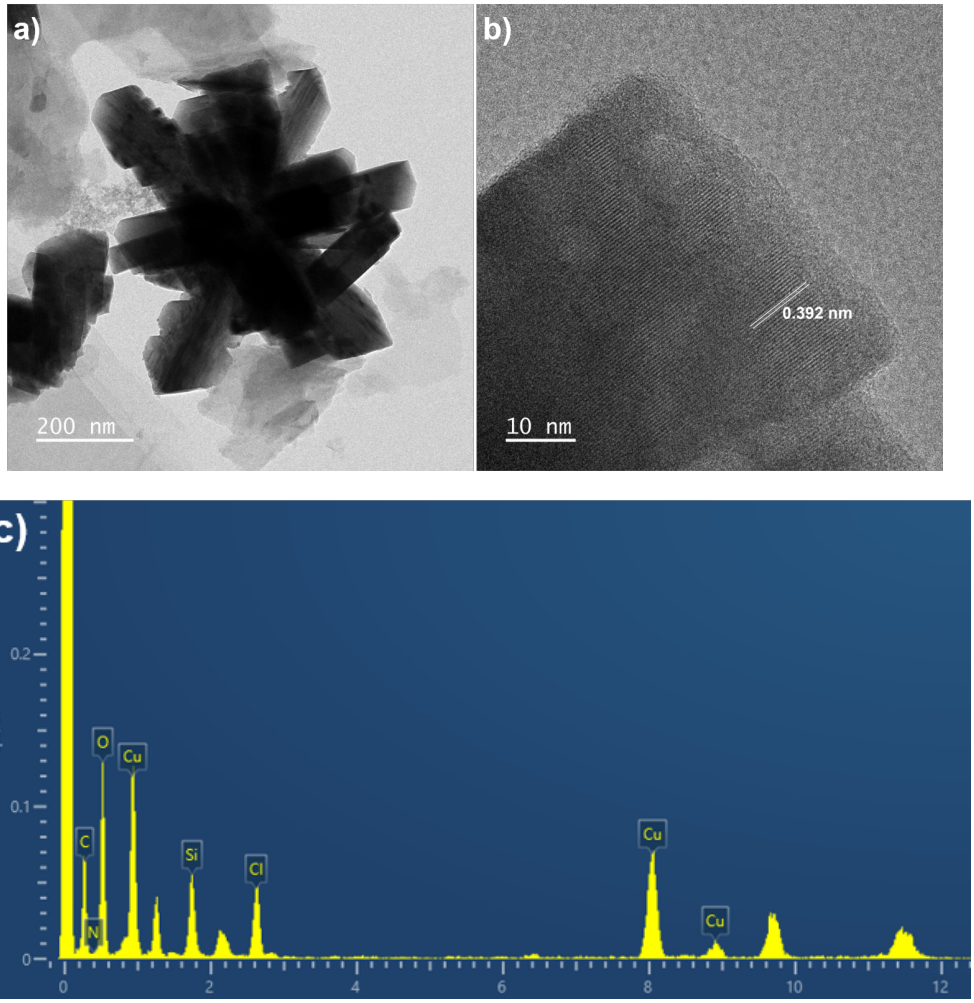

Fig. S2 (a) TEM (b) HR-TEM (c) An energy dispersive analysis of X-rays (EDAX) of ESP-PEI-Cu$^{I/II}$O-NS.

Table S1 TEM-EDAX measurement of ESP-PEI-$Cu^{I/II}$O-NS.

Elements	k-factor	Weight (%)
Carbon (C)	2.659	30.50
Oxygen (O)	1.957	25.15
Nitrogen (N)	3.391	0
Copper (Cu)	1.359	28.02
Chlorine (Cl)	1.033	8.61
Silicon (Si)	1.000	7.71

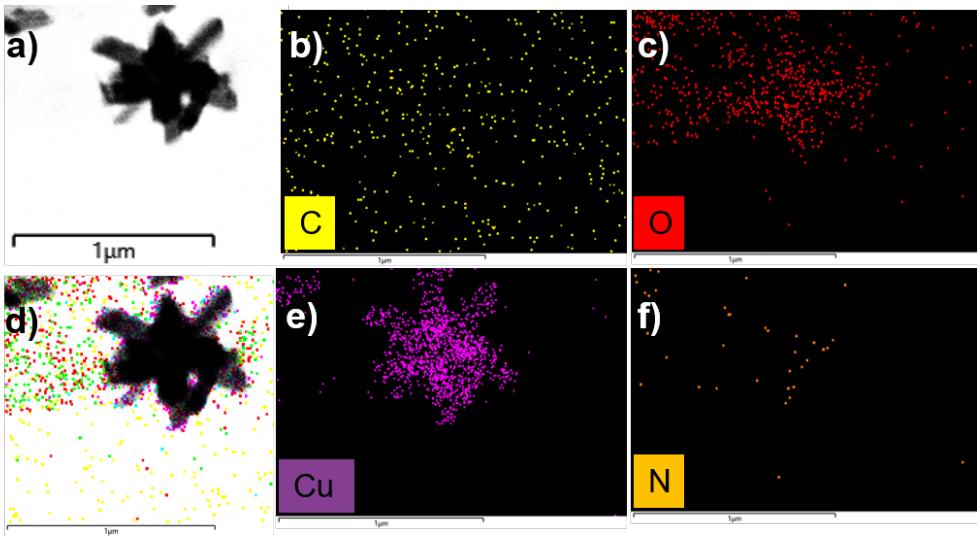

Fig. S3 (a) TEM image of ESP-PEI-$Cu^{I/II}$O-NS portion selected for mapping, (b) C, (c) O, (d) Overlapped image, (e) Cu, (f) N.

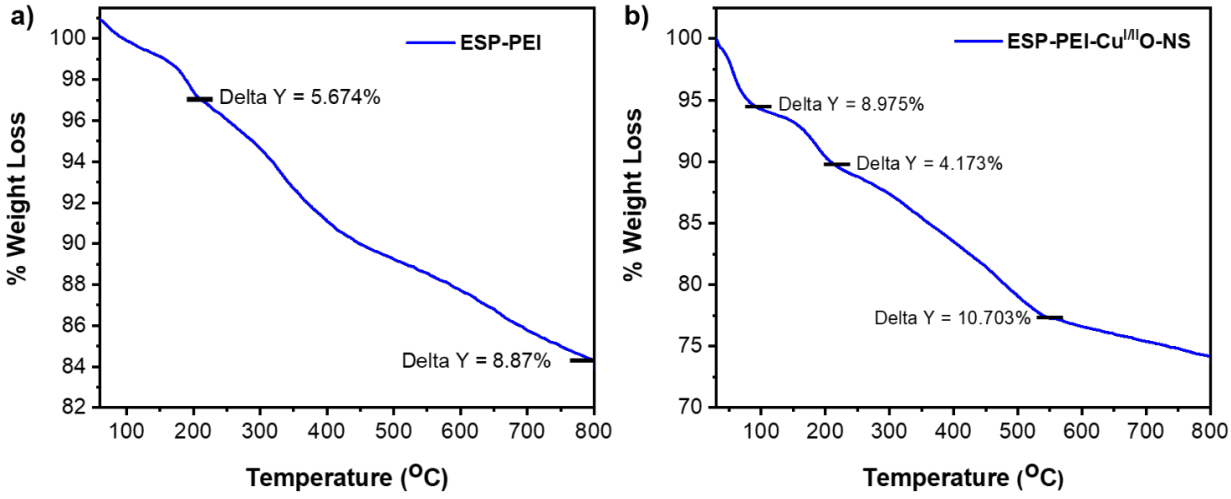

Fig. S4 TGA decomposition pattern of (a) ESP-PEI (b) ESP-PEI-$Cu^{I/II}$O-NS.

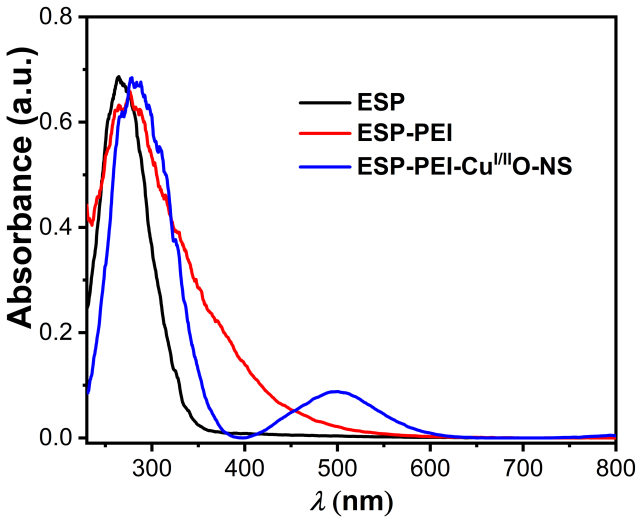

Fig. S5 Comparative diffuse UV/Vis reflectance spectra of ESP, ESP-PEI**,** ESP-PEI-Cu$^{I/II}$O-NS.

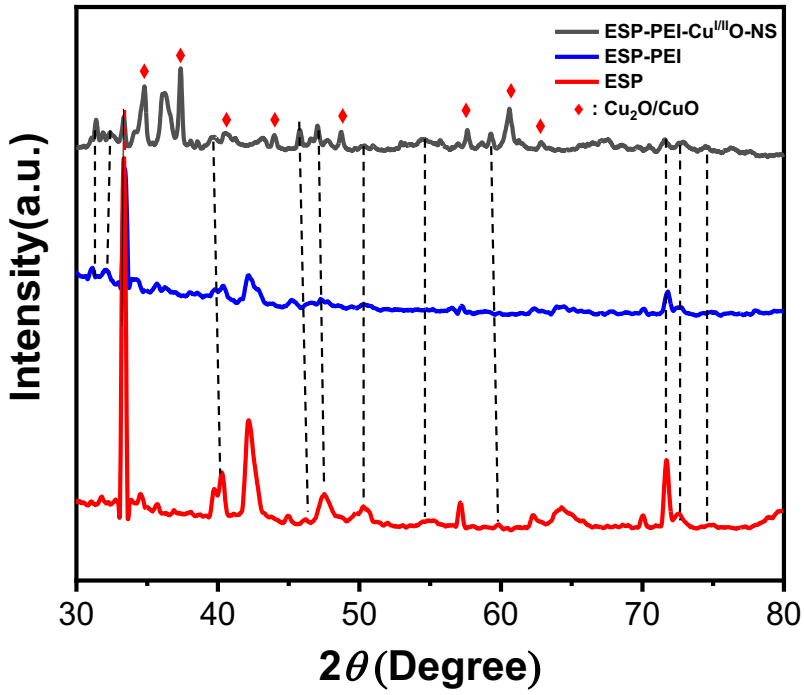

Fig. S6 Overlapped XRD spectra of ESP, ESP-PEI**,** ESP-PEI-Cu$^{I/II}$O-NS.

A time-resolved study of product yield and copper release: In seven separate 10 mL open round-bottom flasks equipped with a magnetic stir bar, 2 mL of H_2O, azide **1b** (0.134 mmol), and alkyne **2a** (0.134 mmol) were added. Additionally, ESP-PEI-Cu$^{I/II}$O-NS (2 mg) was introduced into each flask. The reaction mixtures were stirred at 25 ºC for varying durations (6–24 h). Afterwards, the product was isolated from the reaction mixture by solvent extraction using CH_2Cl_2, and the yield was determined by ^{1}H-NMR spectroscopy, using 1,3,5-trimethoxybenzene as an internal standard. The aqueous layer was then centrifuged to separate

the heterogeneous catalyst, and the supernatant was analyzed by ICP-MS to measure the release of copper.

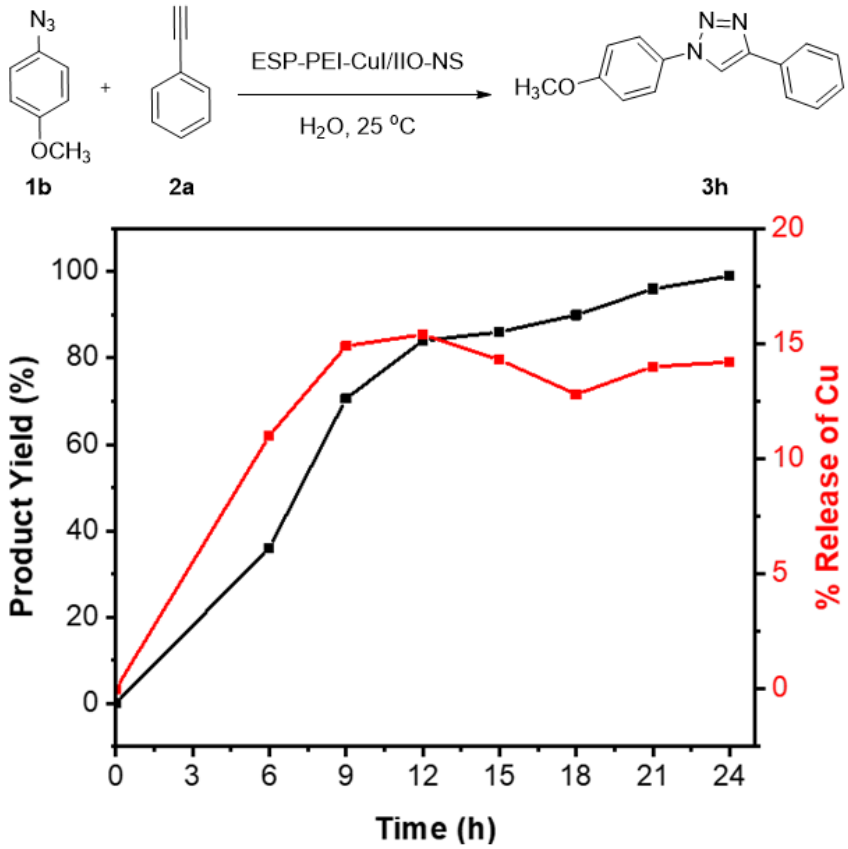

Fig. S7 Graph of copper release versus catalytic product yields over time.

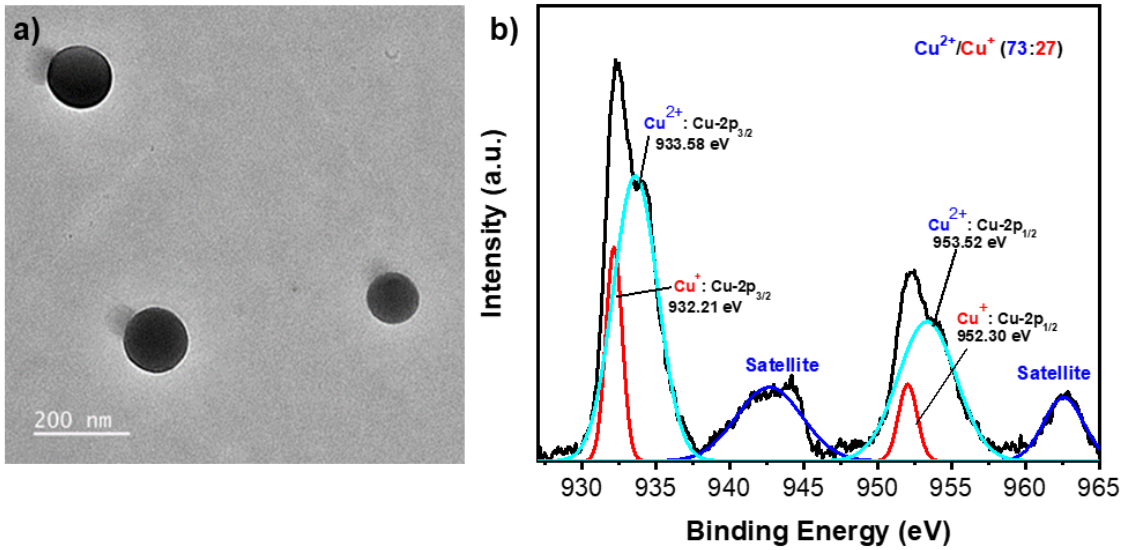

Fig. S8 a) TEM image of reusable ESP-PEI-$Cu^{I/II}$O-NS after 5th cycle, b) XPS of reusable ESP-PEI-$Cu^{I/II}$O-NS after 5th cycle.

Section D:

i) Precursors synthesis for CuAAc reaction

Synthesis of 2,6-difluorobenzylazide[S2]

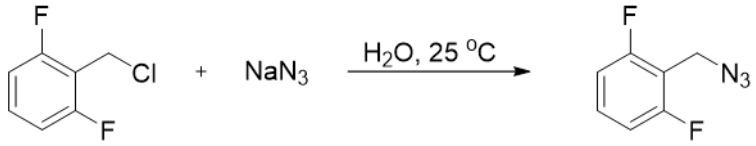

1a. 2,6-difluorobenzylazide was synthesized according to the literature procedure.[S2] Sodium azide (0.349 g, 5.376 mmol) was added in small portions to 2,6-difluorobenzylchloride (1 g, 4.8 mmol) in H_2O (250 mL) at 40 ºC. Then the reaction mixture was stirred at 75 ºC for 14 h, and then cooled to 25 ºC. The aqueous layer was extracted with CH_2Cl_2 (3 × 300 mL). The combined organic layers were washed with water and brine, dried over anhydrous Na_2SO_4, and evaporated to afford **1a** (0.79 g, 97.4%) as an oily liquid.

Synthesis of 4-methoxyphenylazide[S3]

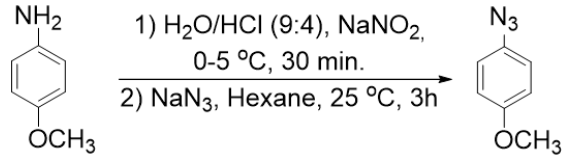

1b. *p*-Anisidine (1g, 0.008 mol) was dissolved in H_2O/HCl 9:4 in a round bottom flask and stirred at 0-5 ºC. $NaNO_2$ (551 mg, 0.008 mol) dissolved in H_2O and was added dropwise to the flask with continuous stirring then aqueous solution of NaN_3 (520 mg, 0.008 mol) was added to the reaction mixture and was allowed to stir at 25 ºC for 2 h. The resultant mixture was extracted with CH_2Cl_2 and washed successively with H_2O (3×100 mL). Organic layer was dried over anhydrous Na_2SO_4 and the solvent was evaporated to afford **1b** (0.96 g, 80.7%) as a yellow liquid.

Synthesis of phenylazide [S3]

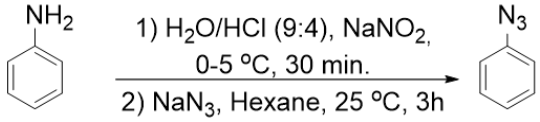

1c. Aniline (1.47 mL, 16 mmol) was dissolved in H_2O (25 mL) and conc. H_2SO_4 (5 mL) was added at 0 °C. Then $NaNO_2$ (1.28 g, 18.5 mmol) dissolved in H_2O (7 mL) was added dropwise. Followed by hexane (24 mL), and NaN_3 (1.26 g, 19.3 mmol) in H_2O (10 mL) was added and the reaction was stirred for 3 h at 25 ºC. The organic phase was separated, washed with H_2O (3 × 50 mL), dried with $MgSO_4$ and filtered. The solvent was removed in vacuo, yielding compound **1c** (1.44 g, 75.4%) as pale-yellow oil.

ii) General procedure for ESP-PEI-Cu$^{I/II}$O-NS catalyzed azide-alkyne cycloaddition reaction

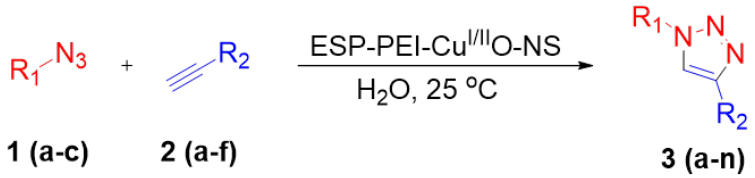

1 (a-c) **2 (a-f)** **3 (a-n)**

A 10 mL open round-bottom flask with a magnetic stir bar was charged with 1 mL of H_2O, azide **1a-c** (1.0 equiv.), alkyne **2a-e** (1.0 equiv.) and ESP-PEI-Cu$^{I/II}$O-NS (1 mg) was added. The reaction mixture was allowed to stir at 25 ºC and reaction was monitored through thin-layer chromatography (TLC). After completion of the reaction, the product was separated from the reaction mixture by the solvent extraction in CH_2Cl_2 (3 × 10 mL), washed with H_2O and the organic layer was dried over anhydrous Na_2SO_4. The solvent was removed *in vacuo* to yield the triazole **3a-n** product.

iii) Spectral details of triazole products:

1-(2,6-difluorobenzyl)-4-phenyl-1H-1,2,3-triazole

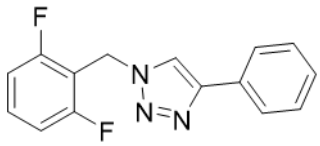

3a.[S4] ^{1}H NMR (400 MHz, $CDCl_3$): δ = 5.67 (s, 2H), 6.99 (t, J = 7.88 Hz, 2H), 7.29-7.32 (m, 1H), 7.35-7.41 (m, 3H), 7.78 (d, J = 6.6 Hz, 2H), 7.81 ppm (s, 1H); ^{13}C NMR (100 MHz, $CDCl_3$): δ = 41.59 (t, $^3J_{CF}$ = 3.97 Hz), 111.03 (t, $^3J_{CF}$ = 18.77 Hz), 111.87-112.13 (m), 119.62, 125.89, 128.31, 128.92, 130.62, 131.58 (t, $^3J_{CF}$ = 10.47 Hz) , 148.26, 161.56 ppm (dd, $^1J_{CF}$ = 249.86, Hz, $^3J_{CF}$ = 6.91 Hz)

1-(2,6-difluorobenzyl)-4-(p-tolyl)-1H-1,2,3-triazole

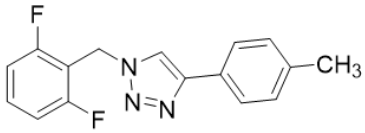

3b.[S2] ^{1}H NMR (400 MHz, $CDCl_3$): δ = 2.36 (s, 3H), 5.66 (s, 2H), 6.96-7.00 (m, 2H), 7.20 (d, J = 7 Hz, 2H), 7.32-7.41 (m, 1H), 7.69 (d, J = 8.12 Hz, 2H), 7.73 ppm (s, 1H); ^{13}C NMR (100 MHz, $CDCl_3$): ^{13}C NMR (100 MHz, DMSO-d_6): δ = 21.37, 41.51 (t, $^3J_{CF}$ = 3.97 Hz),111.07 ($^3J_{CF}$ = 18.78 Hz), 111.86-112.11 (m), 119.26, 125.78, 127.80, 129.67, 131.54 (t, $^3J_{CF}$ = 10.11 Hz), 138.14, 148.33, 161.59 ppm (dd, $^1J_{CF}$ = 6.86, $^3J_{CF}$ = 7.29 Hz).

methyl 1-(2,6-difluorobenzyl)-1H-1,2,3-triazole-4-carboxylate

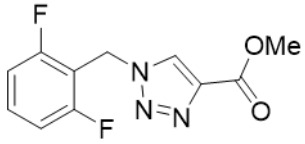

3c.[S2] ^{1}H NMR (400 MHz, DMSO-d_6): δ = 3.82 (s, 3H), 5.74 (s, 2H), 7.18 (t, J = 8.28, 2H), 7.49-7.56 (m,1H), 8.85 ppm (s, 1H); ^{13}C NMR (100 MHz, DMSO-d_6): δ = 41.35 (t, $^{3}J_{CF}$ = 3.61 Hz), 51.83, 110.83 (t, $^{3}J_{CF}$ = 18.77 Hz), 11.85-112.09 (m), 129.47, 131.90 (t, $^{3}J_{CF}$ = 10.47 Hz), 138.49, 160.56, 160.81 ppm (dd, $^{3}J_{CF}$ = 248.02, $^{3}J_{CF}$ = 7.29 Hz).

1-(2,6-difluorobenzyl)-4-(4-methoxyphenyl)-1H-1,2,3-triazole

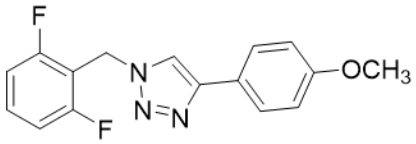

3d. ^{1}H NMR (400 MHz, $CDCl_3$): δ = 3.83 (s, 3H), 5.66 (s, 2H), 6.92-7.00 (m, 4H), 7.33-7.41 (m, 1H), 7.69-7.74 ppm (m, 3H); ^{13}C NMR (100 MHz, $CDCl_3$): δ = 41.50 (t, $^{3}J_{CF}$ = 3.97 Hz), 55.45, 111.10 (t, $^{3}J_{CF}$ = 15.88 Hz), 11.86-112.12 (m), 114.33, 118.82, 123.37, 127.20, 131.54 (t, $^{3}J_{CF}$ = 10.47 Hz) , 148.13, 159.76, 161.57 ppm (dd, $^{1}J_{CF}$ =279.96, $^{3}J_{CF}$ = 6.86 Hz).

4-(4-chlorophenyl)-1-(2,6-difluorobenzyl)-1H-1,2,3-triazole

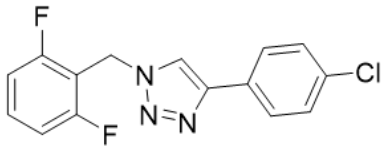

3e. ^{1}H NMR (400 MHz, $CDCl_3$): δ = 5.67 (s, 2H), 6.99 (t, J = 7.88 Hz, 2H), 7.35-7.42 (m, 3H), 7.73-7.77 ppm (m, 3H); ^{13}C NMR (100 MHz, $CDCl_3$): δ = 41.93 (t, $^{3}J_{CF}$ = 3.97 Hz) , 112.23-112.49 (m),120.01, 127.27, 127.45, 129.44, 131.99 (t, $^{3}J_{CF}$ = 10.01 Hz) ,134.39, 135.38, 147.55, 163.12 ppm (dd, $^{1}J_{CF}$ = 249.82, $^{3}J_{CF}$ = 6.86 Hz).

4-(4-bromophenyl)-1-(2,6-difluorobenzyl)-1H-1,2,3-triazole

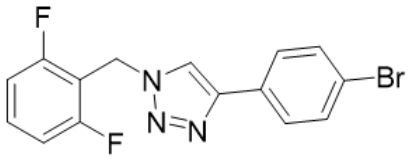

3f. ^{1}H NMR (400 MHz, $CDCl_3$): δ = 5.67 (s, 2H), 6.99 (t, J = 7.64 Hz, 2H), 7.34-7.41 (m, 1H), 7.52 (d, J = 8.48 Hz, 2H), 7.68 (d, J = 8.40 Hz, 2H), 7.74 (s,1H) ppm; ^{13}C NMR (100 MHz, $CDCl_3$): δ = 41.61 (t, $^{3}J_{CF}$ = 3.97 Hz),110.88 (t, $^{3}J_{CF}$ = 18.77 Hz), 111.90-112.16 (m), 119.72, 122.28, 127.40, 129.59, 131.67 (t, $^{3}J_{CF}$ = 10.10 Hz) ,132.07, 147.22, 161.53 ppm (dd, $^{3}J_{CF}$ = 249.82, Hz $^{3}J_{CF}$ = 6.50 Hz).

methyl 1-(4-methoxyphenyl)-1H-1,2,3-triazole-4-carboxylate

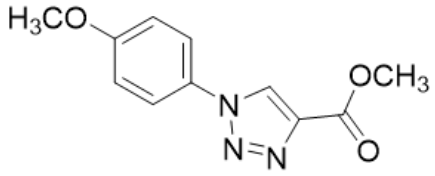

3g.[S5] ^{1}H NMR (400 MHz, $CDCl_3$): δ = 3.88 (s, 3H), 3.99 (s, 3H), 7.04 (d, J = 9.00 Hz, 2H), 7.65 (d, J = 9 Hz, 2H), 8.42 ppm (s, 1H); ^{13}C NMR (100 MHz, $CDCl_3$): δ = 52. 78, 56.05, 115.42, 122.93, 126.07, 130.15, 140.82, 160.86, 161.60 ppm.

1-(4-methoxyphenyl)-4-phenyl-1H-1,2,3-triazole

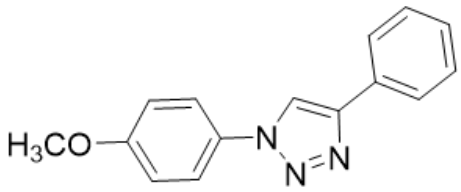

3h.[S6] ^{1}H NMR (400 MHz, $CDCl_3$): δ = 3.87 (s, 3H), 7.03 (d, J =8.88 Hz, 2H), 7.34-7.38 (m, 1H), 7.43-7.47 (m, 2H), 7.68 (d, J = 8.88, 2H), 7.90 (d, J = 7.88 Hz, 2H), 8.12 ppm (s, 1H); ^{13}C NMR (100 MHz, $CDCl_3$): δ = 55.78, 114.93, 117.97, 122.32, 125.95, 128.46, 128.95, 130.52, 130.67, 148.35, 159.98 ppm.

1,4-bis(4-methoxyphenyl)-1H-1,2,3-triazole

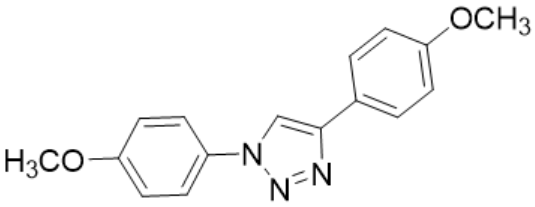

3i.[S7] ^{1}H NMR (400 MHz, $CDCl_3$): δ = 3.87(d, J = 7.36 Hz, 6H), 6.98-7.65 (m, 4H), 7.68 (d, J = 9 Hz, 2H), 7.83 (d, J = 8.76 Hz, 2H), 8.02 ppm (s, 1H); ^{13}C NMR (100 MHz, $CDCl_3$): δ = 55.50, 55.80, 114.47, 114.93, 117.17, 122.31, 123.24, 127.29, 130.79, 148.25, 159.90, 159.94 ppm.

1-(4-methoxyphenyl)-4-(p-tolyl)-1H-1,2,3-triazole

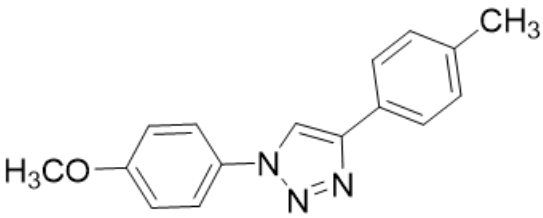

3j.[S8] ^{1}H NMR (400 MHz, $CDCl_3$): δ = 2.37 (s, 3H), 3.86 (s, 3H), 7.02 (d, J = 9.00 Hz, 2H), 7.25 (d, J = 5.72 Hz, 2H), 7.67 (d, J = 9.00 Hz, 2H), 7.78 (d, J = 8.12 Hz, 2H), 8.06 ppm (s, 1H); ^{13}C NMR (100 MHz, $CDCl_3$): δ = 21.44, 55.76, 114.90, 117.61, 122.28, 125.85, 127.69, 129.70, 130.72, 138.32, 148.42, 159.92 ppm.

4-(4-bromophenyl)-1-(4-methoxyphenyl)-1H-1,2,3-triazole

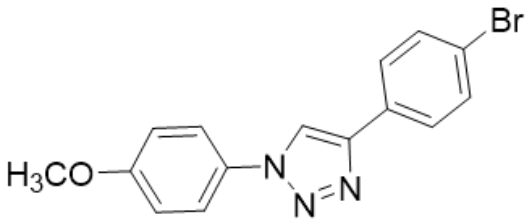

3k.[S9] ^{1}H NMR (400 MHz, DMSO-d_6): δ = 3.84 (s, 3H), 7.18 (d, J = 9.00 Hz, 2H), 7.71 (d, J = 8.52 Hz, 2H), 7.83-7.90 (m, 4H), 9.26 ppm (s, 1H); ^{13}C NMR (100 MHz, DMSO-d_6): δ = 55.66, 115.01, 120.10, 121.23, 121.77, 127.30, 129.70, 130.01, 132.06, 146.12, 159.43 ppm.

4-(4-chlorophenyl)-1-(4-methoxyphenyl)-1H-1,2,3-triazole

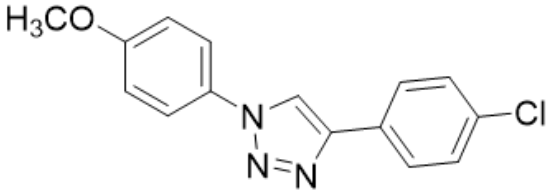

3l.[S7] ^{1}H NMR (400 MHz, DMSO-d_6): δ = 3.85 (s, 3H), 7.18 (d, J = 9.12 Hz, 2H), 7.58 (d, J = 8.52 Hz, 2H), 7.85 (d, J = 9.16 Hz, 2H), 7.95 (d, J = 6.48 Hz, 2H), 9.26 ppm (s, 1H); ^{13}C NMR (100 MHz, DMSO-d_6): δ = 55.67, 115.02, 120.10, 127.79, 127.03, 129.17, 129.36, 130.03, 132.65, 146.09, 159.44 ppm.

1,4-diphenyl-1H-1,2,3-triazole

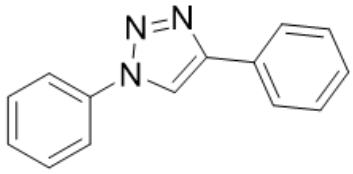

3m.[S10] ^{1}H NMR (400 MHz, DMSO-d_6): δ = 7.37-7.41 (m, 1H), 7.49-7.54 (m, 3H), 7.62-7.65 (m, 2H), 7.96 (d, J = 8.36 Hz, 4H), 9.30 ppm (s, 1H); ^{13}C NMR (100 MHz, DMSO-d_6): δ = 119.63, 120.03, 125.36, 128.27, 128.74, 129.01, 129.96, 130.26, 136.66, 147.34 ppm.

methyl 1-phenyl-1H-1,2,3-triazole-4-carboxylate

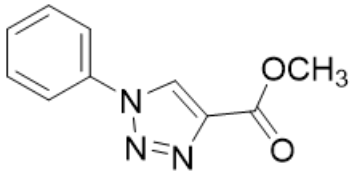

3n.[S11] ^{1}H NMR (400 MHz, $CDCl_3$): δ = 4.00 (s, 3H), 7.48-7.58 (m, 3H), 7.76 (d, J = 7.24 Hz, 2H), 8.52 (s, 1H) ppm; ^{13}C NMR (100 MHz, $CDCl_3$): δ = 52.52, 120.98, 125.70, 129.72, 130.01, 136.50, 140.72, 161.20 ppm.

[1]H-, [13]C-NMR and mass spectral profiles of triazole-products

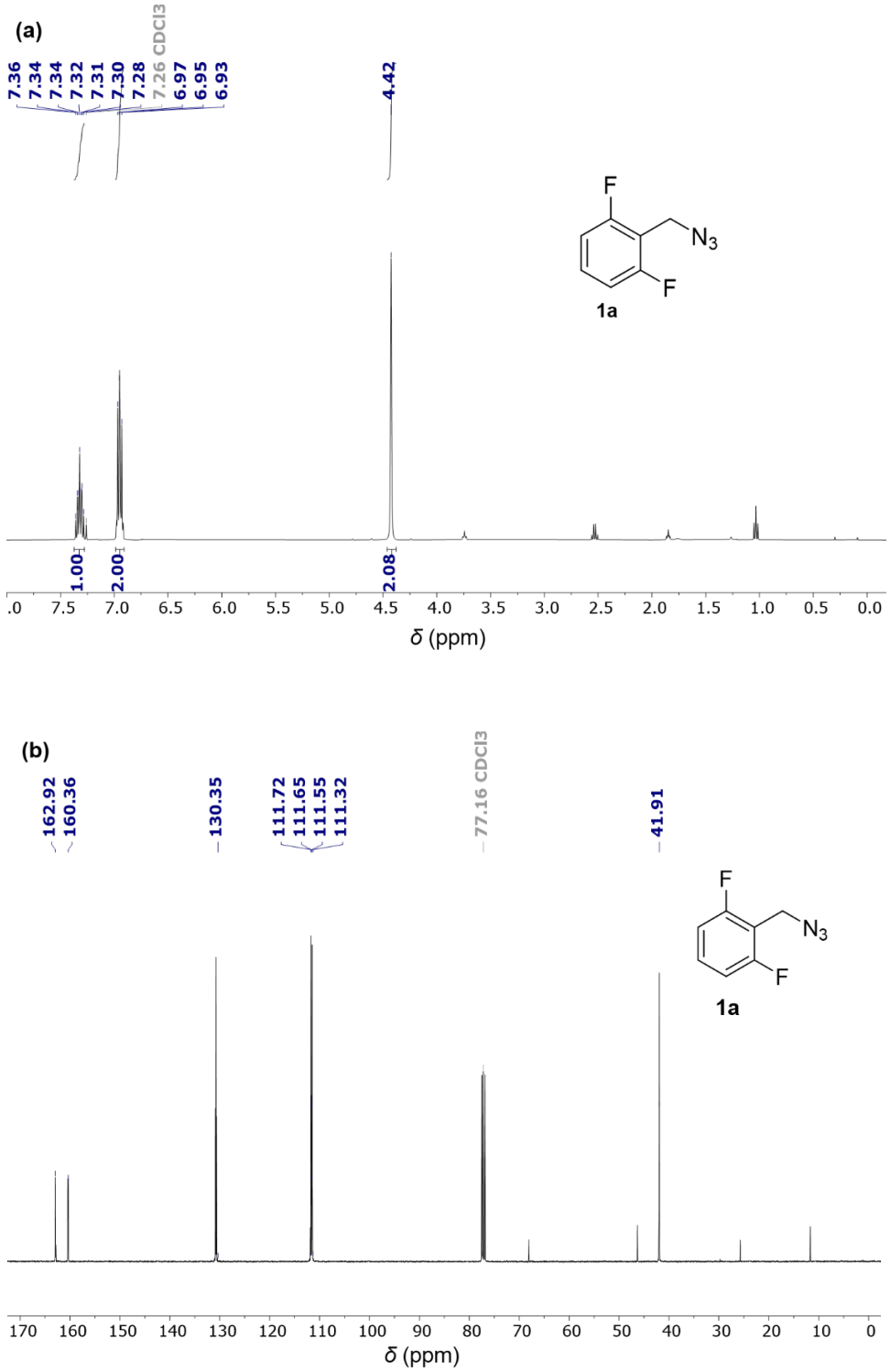

Fig. S9 (a) ^{1}H-NMR (400 MHz, $CDCl_3$, 298 K), (b) ^{13}C-NMR (100 MHz, $CDCl_3$, 298 K) spectra of **1a**.

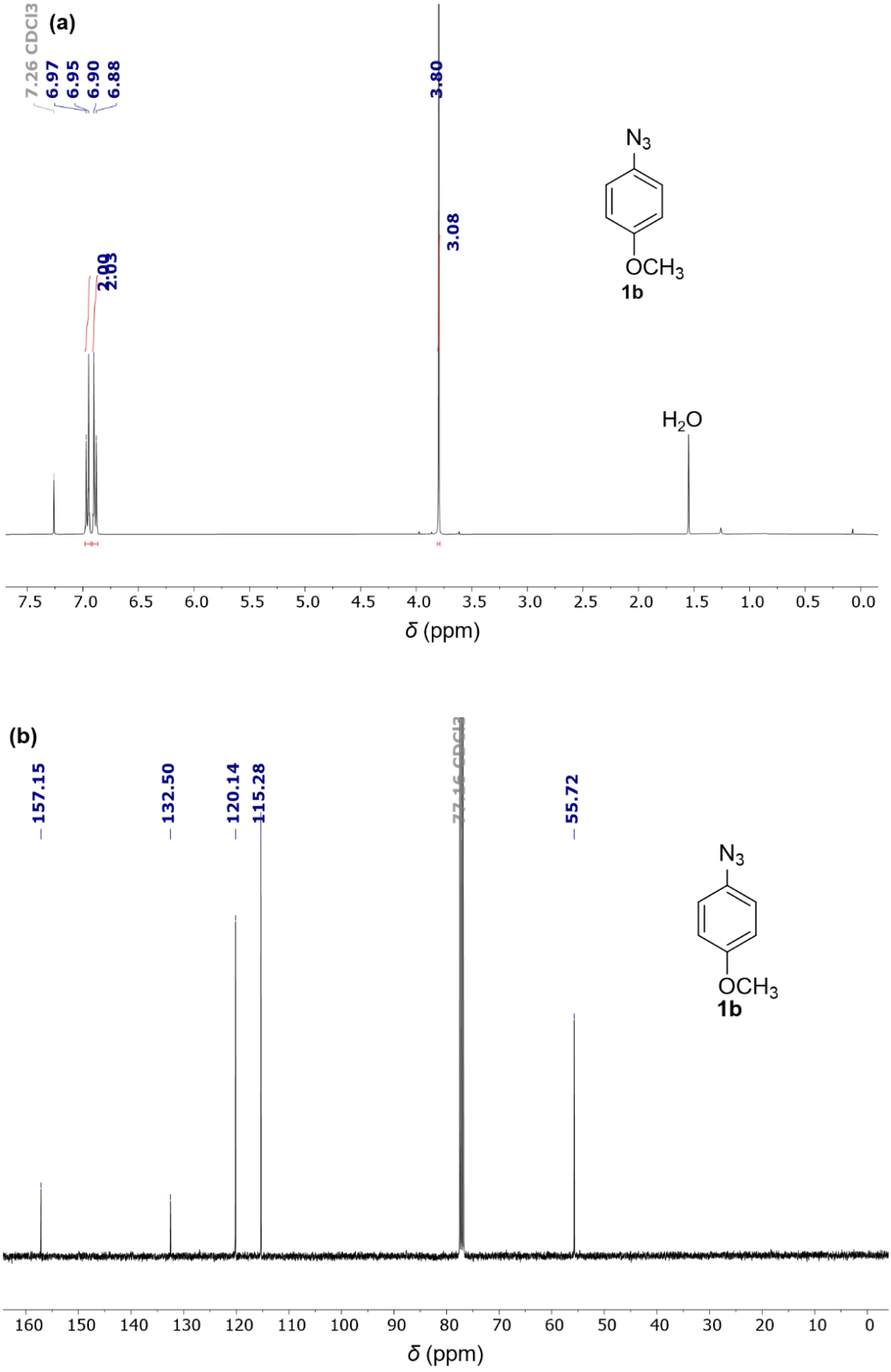

Fig. S10 (a) ^{1}H-NMR (400 MHz, $CDCl_3$, 298 K), (b) ^{13}C-NMR (100 MHz, $CDCl_3$, 298 K) spectra of **1b**.

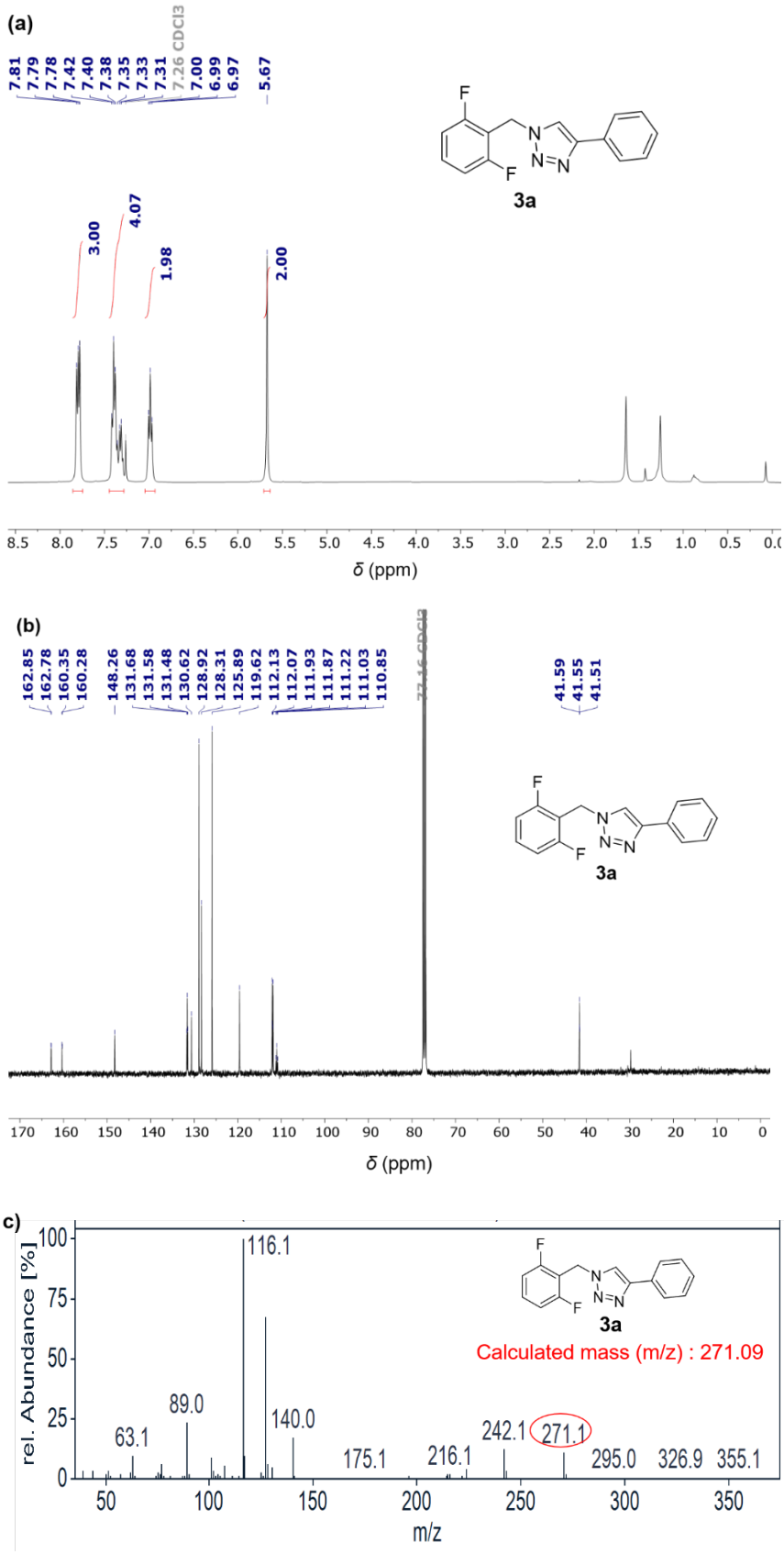

Fig. S11 (a) ^{1}H-NMR (400 MHz, $CDCl_3$, 298 K), (b) ^{13}C-NMR (100) MHz, $CDCl_3$, 298 K), (c) GC-MS spectra of **3a**.

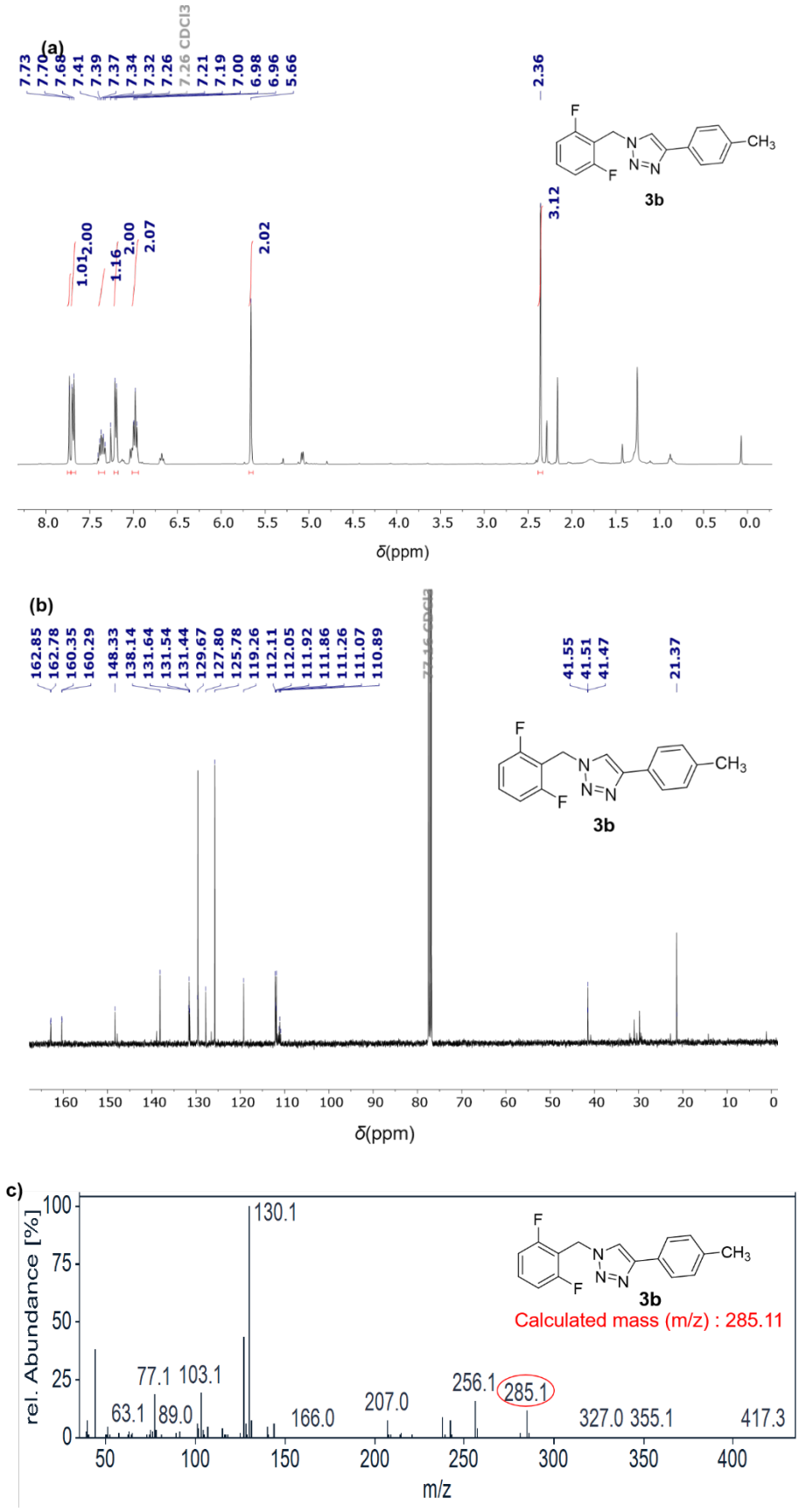

Fig. S12 (a) ^{1}H-NMR (400 MHz, $CDCl_3$, 298 K), (b) ^{13}C-NMR (100 MHz, $CDCl_3$, 298 K), (c) GC-MS spectra of **3b**.

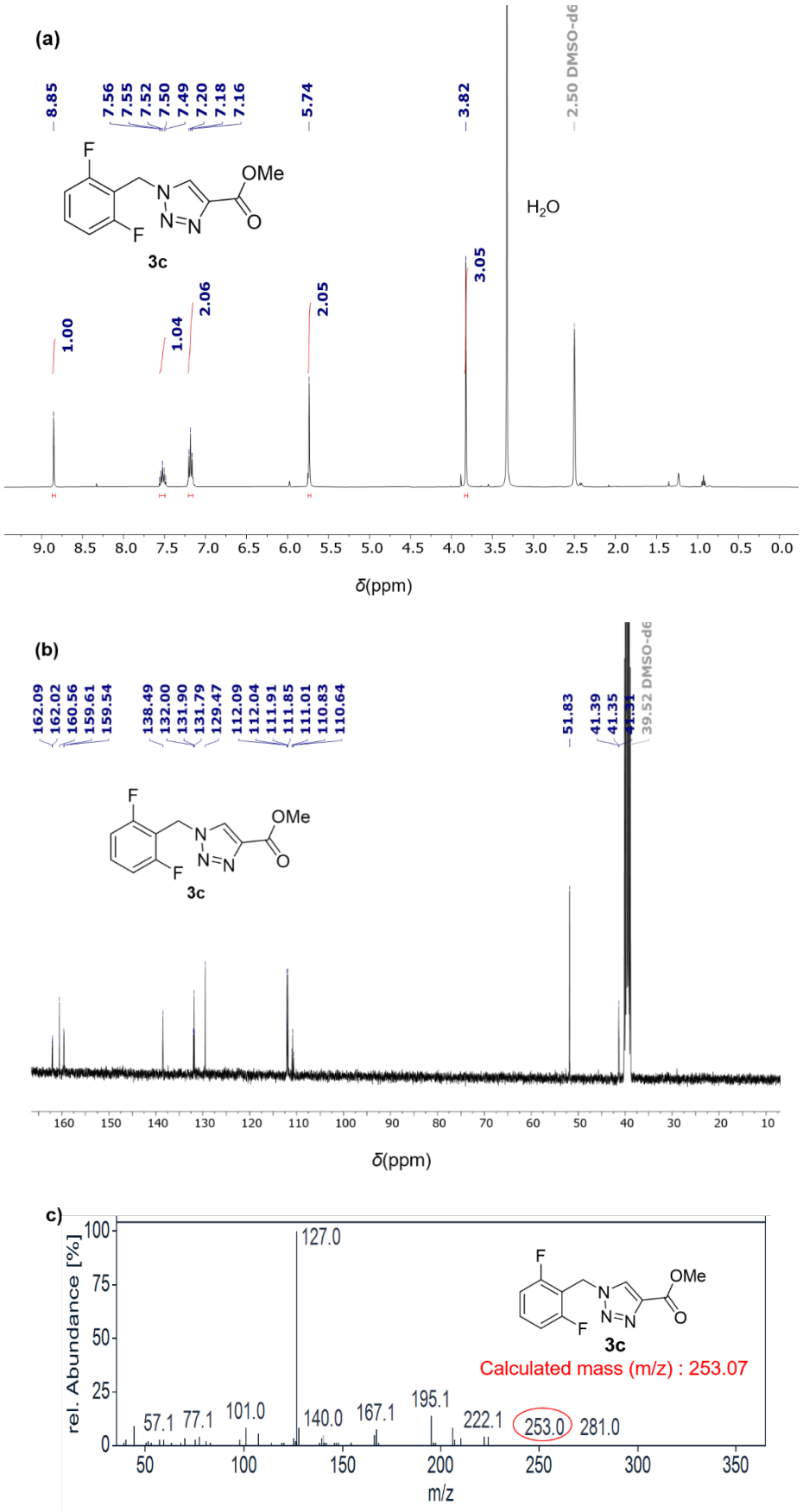

Fig. S13 (a) ^{1}H-NMR (400 MHz, DMSO-d_6, 298 K), (b) ^{13}C-NMR (100 MHz, DMSO-d_6, 298 K, (c) GC-MS spectra of **3c**.

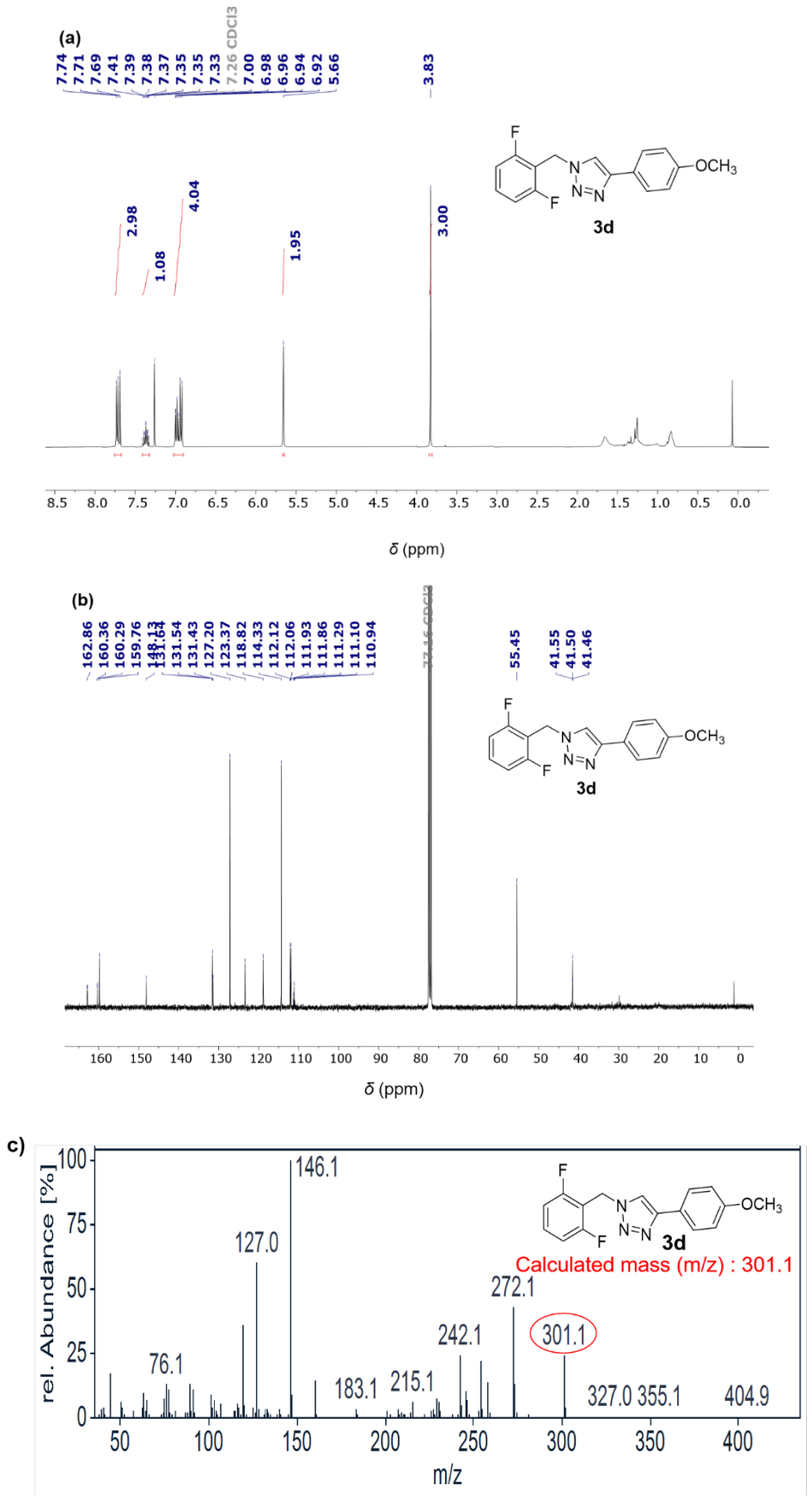

Fig. S14 (a) ^{1}H-NMR (400 MHz, $CDCl_3$, 298 K), (b) ^{13}C-NMR (100 MHz, $CDCl_3$, 298 K, (c) GC-MS spectra of **3d**.

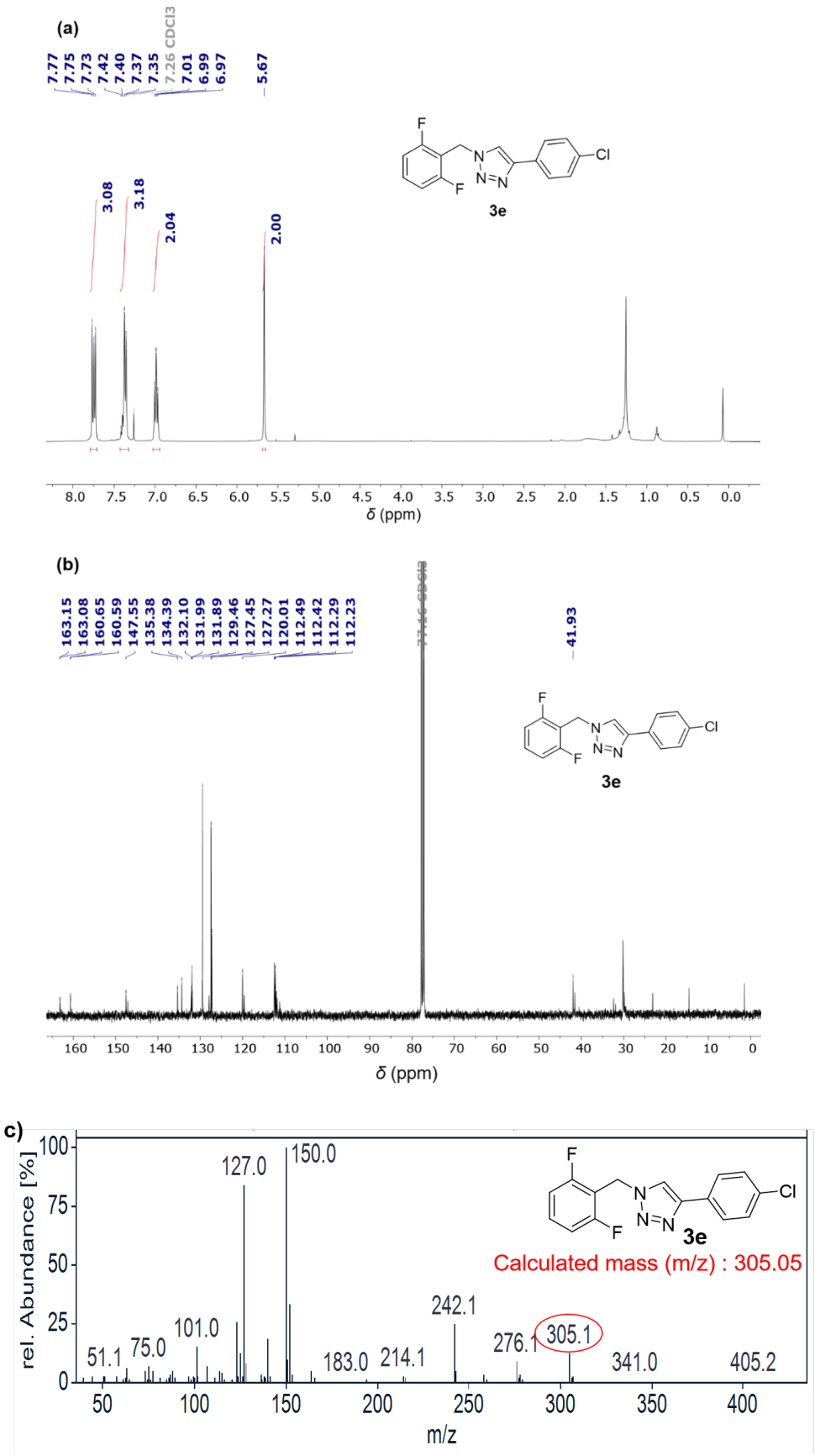

Fig. S15 (a) ^{1}H-NMR (400 MHz, $CDCl_3$, 298 K), (b) ^{13}C-NMR (100 MHz, $CDCl_3$, 298 K, (c) GC-MS spectra of **3e**.

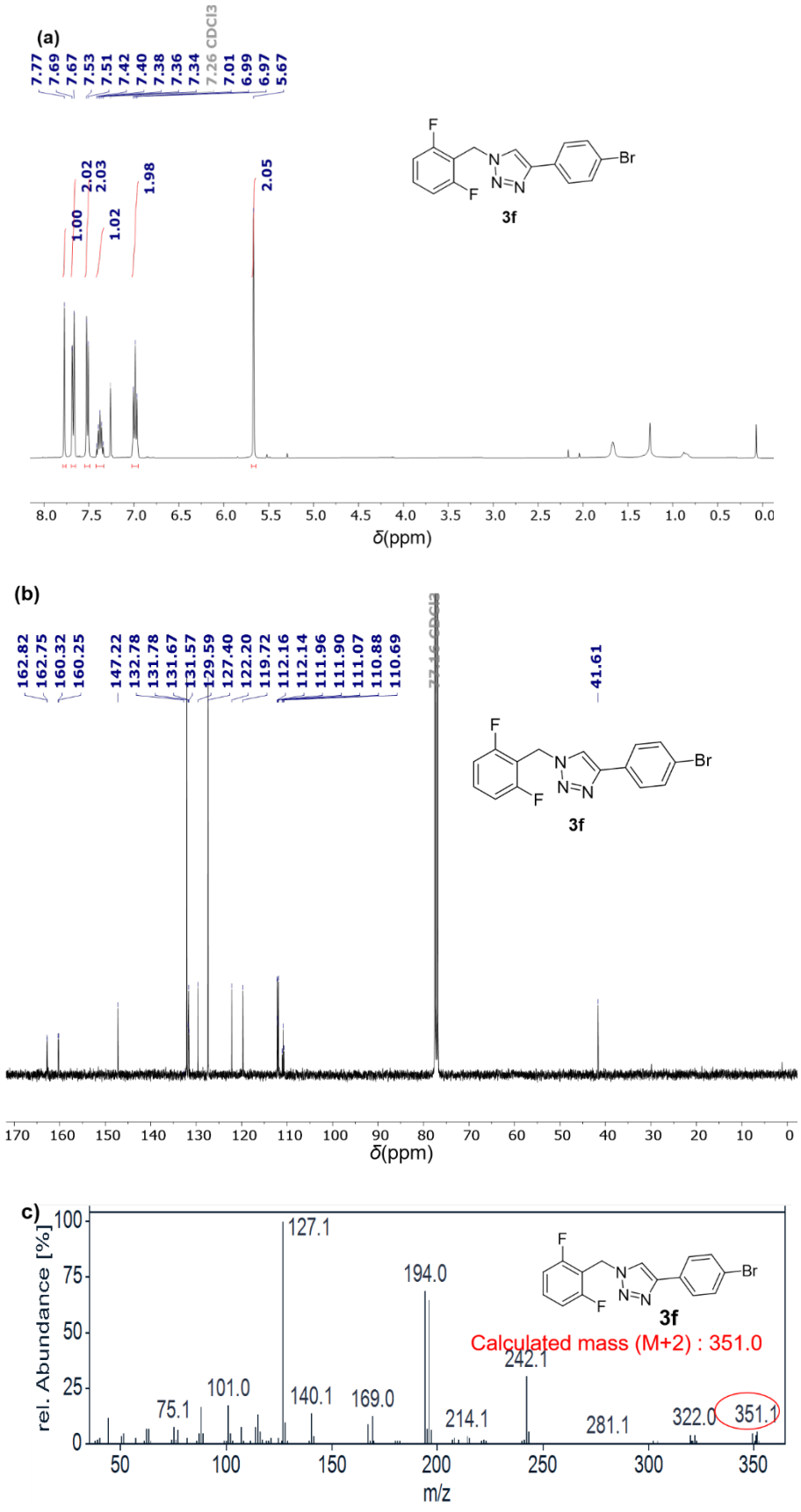

Fig. S16 (a) ^{1}H-NMR (400 MHz, $CDCl_3$, 298 K), (b) ^{13}C-NMR (100 MHz, $CDCl_3$, 298 K, (c) GC-MS spectra of **3f**.

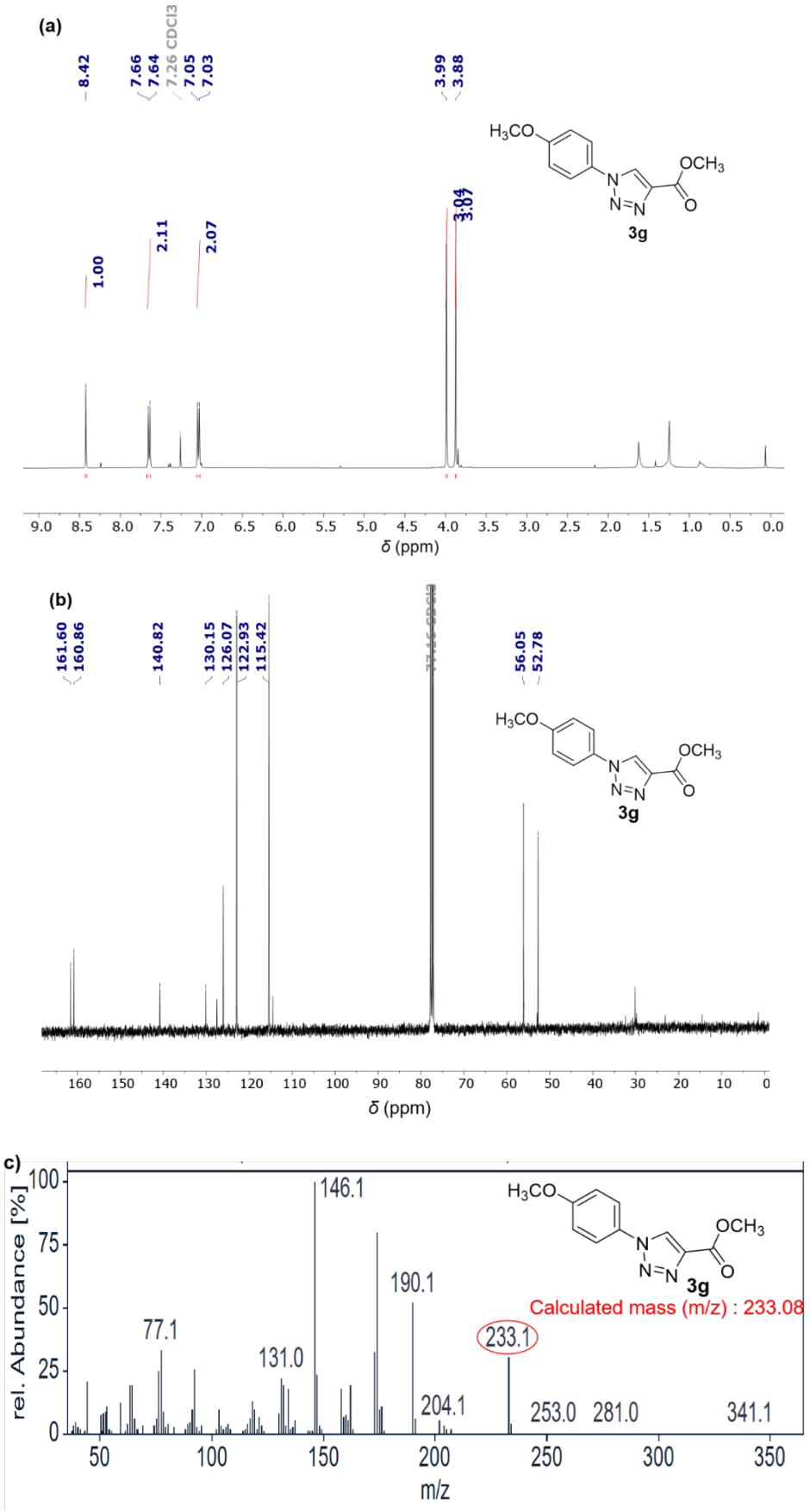

Fig. S17 (a) ^{1}H-NMR (400 MHz, $CDCl_3$, 298 K), (b) ^{13}C-NMR (100 MHz, $CDCl_3$, 298 K, (c) GC-MS spectra of **3g**.

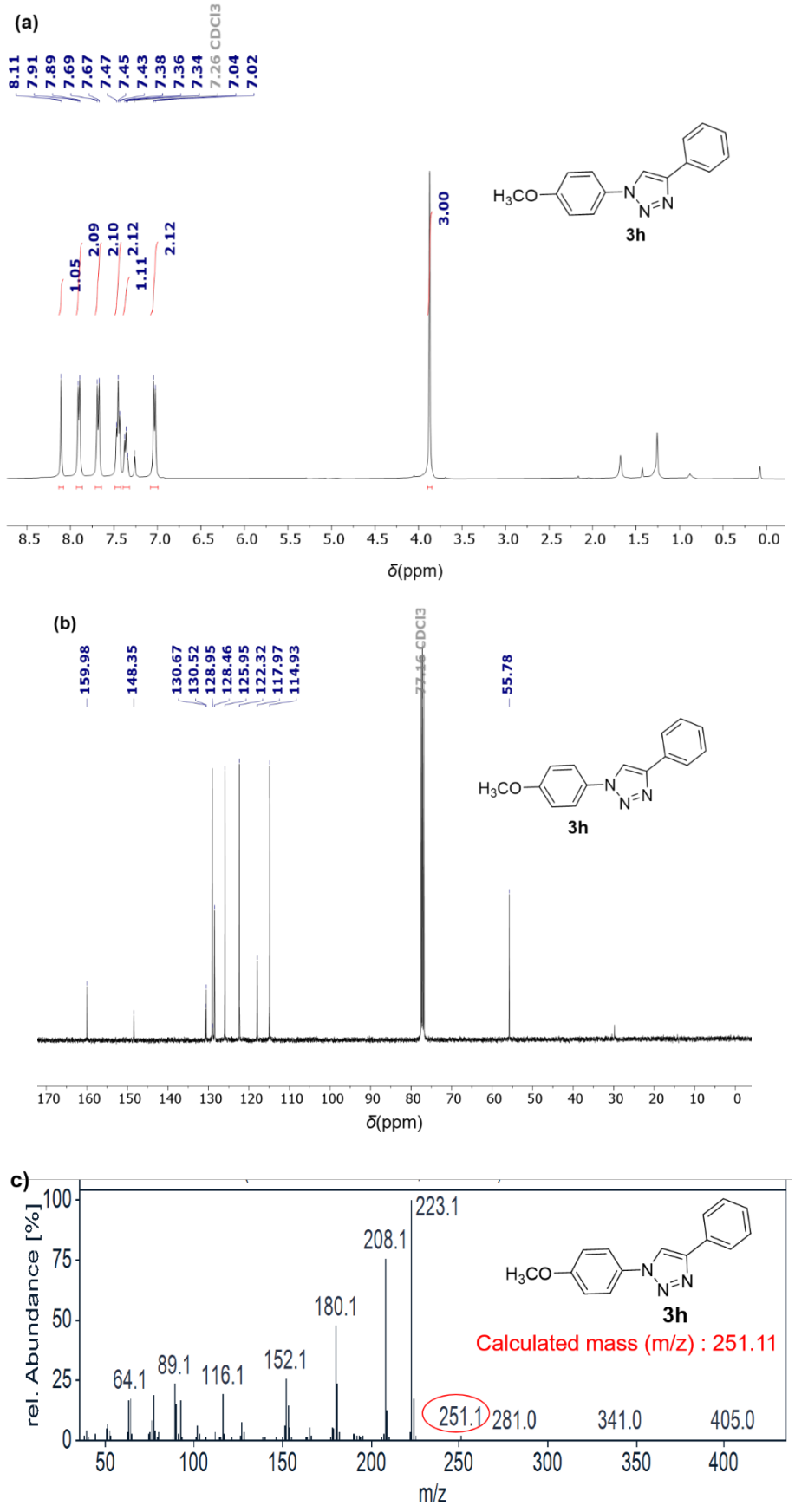

Fig. S18 (a) ^{1}H-NMR (400 MHz, $CDCl_3$, 298 K), (b) ^{13}C-NMR (100 MHz, $CDCl_3$, 298 K, (c) GC-MS spectra of **3h**.

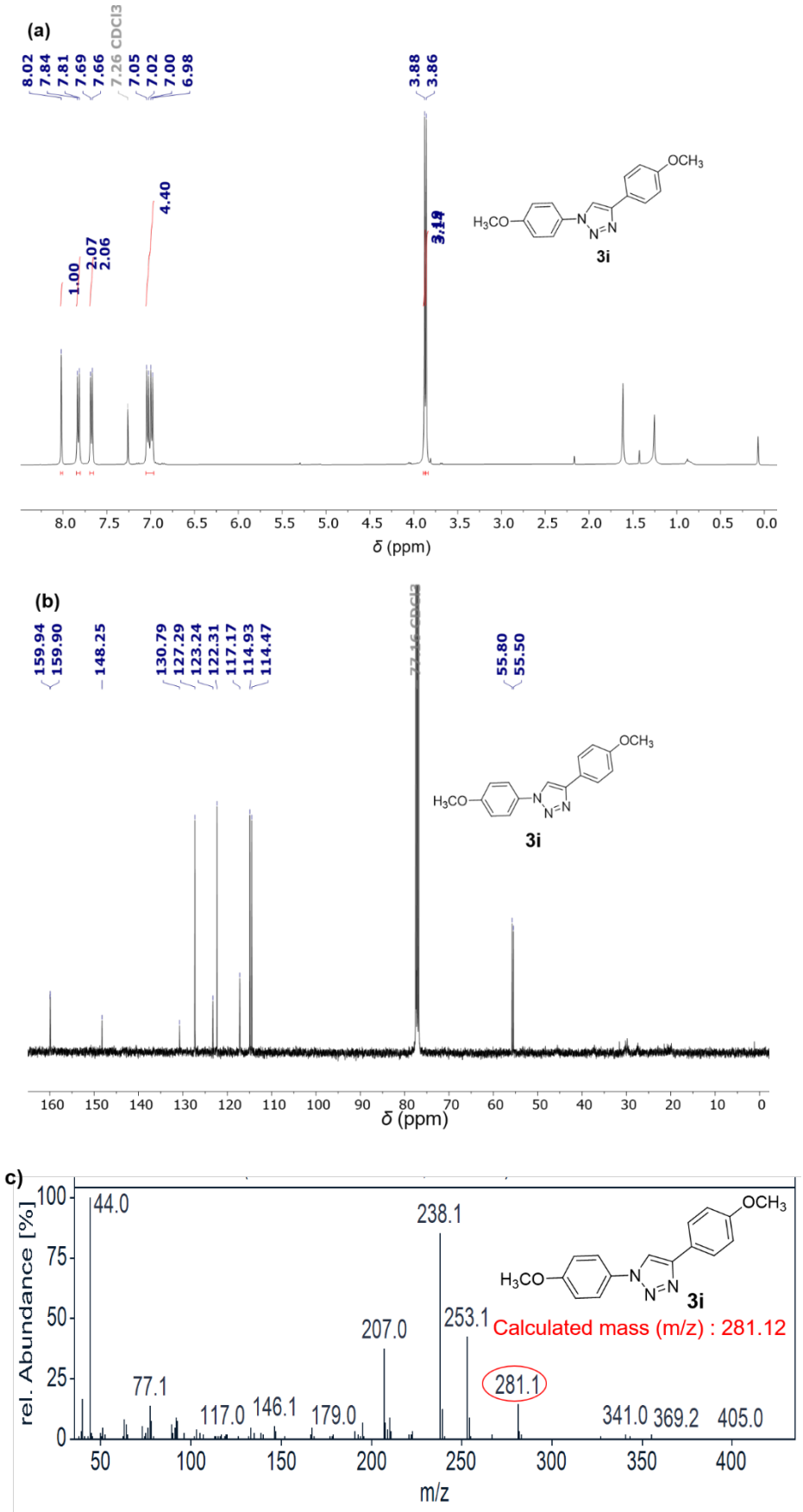

Fig. S19 (a) ^{1}H-NMR (400 MHz, $CDCl_3$, 298 K), (b) ^{13}C-NMR (100 MHz, $CDCl_3$, 298 K, (c) GC-MS spectra of **3i**.

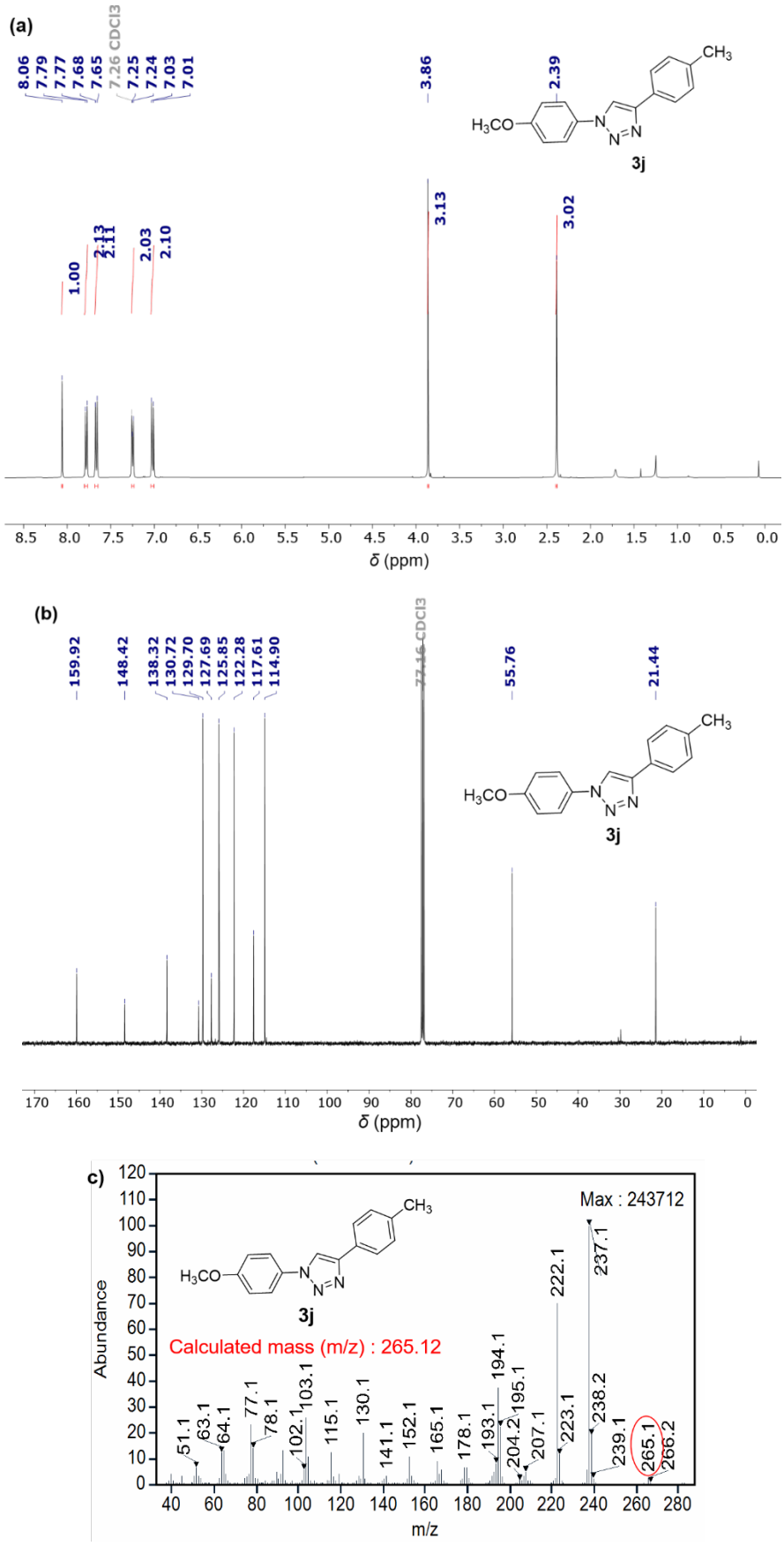

Fig. S20 (a) ^{1}H-NMR (400 MHz, $CDCl_3$, 298 K), (b) ^{13}C-NMR (100 MHz, $CDCl_3$, 298 K, (c) GC-MS spectra of **3j**.

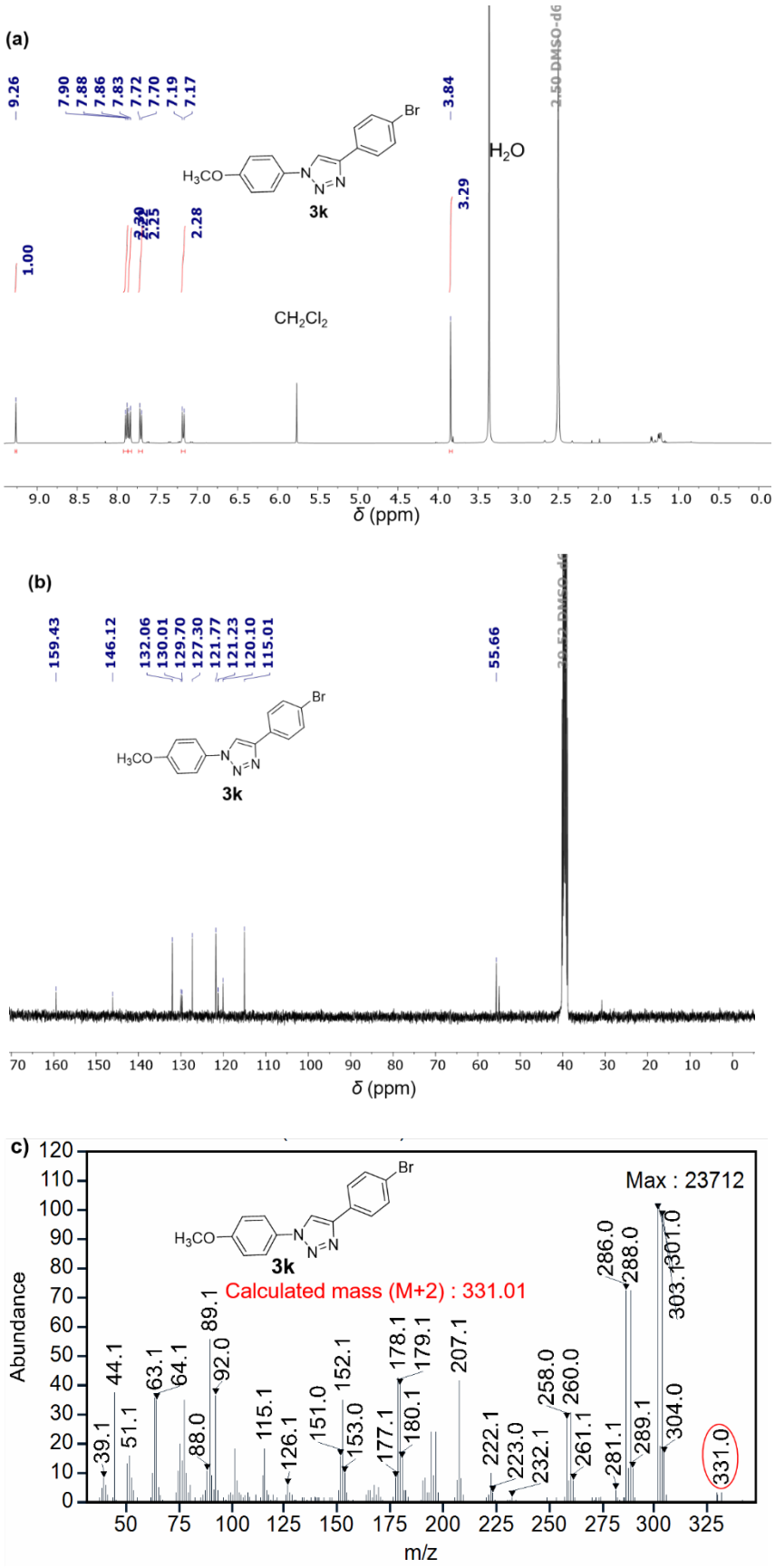

Fig. S21 (a) ^{1}H-NMR (400 MHz, DMSO-d_6, 298 K), (b) ^{13}C-NMR (100 MHz, DMSO-d_6, 298 K, (c) GC-MS spectra of **3k**.

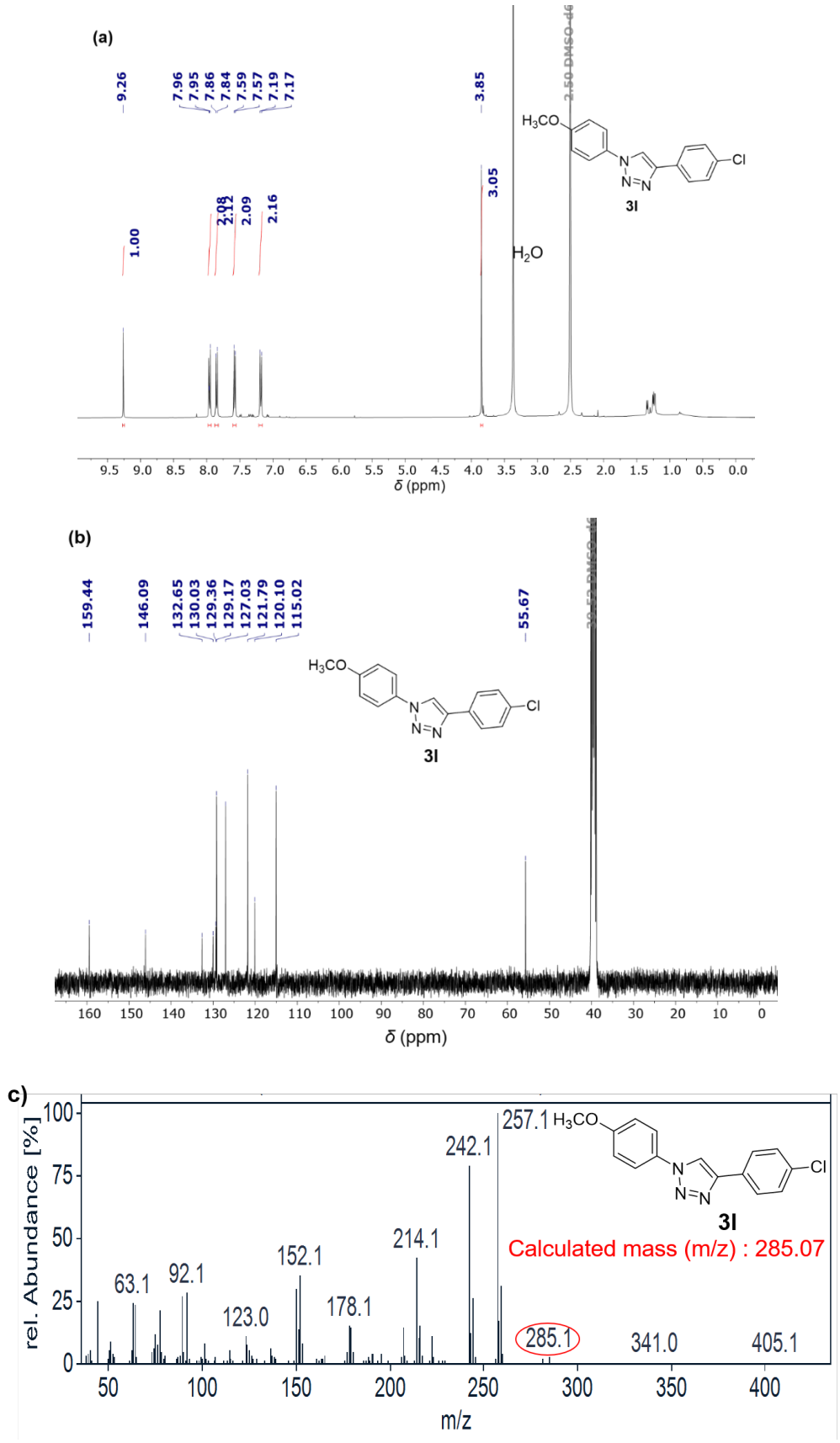

Fig. S22 (a) ^{1}H-NMR (400 MHz, DMSO-d_6, 298 K), (b) ^{13}C-NMR (100 MHz, DMSO-d_6, 298 K, (c) GC-MS spectra of **3l**.

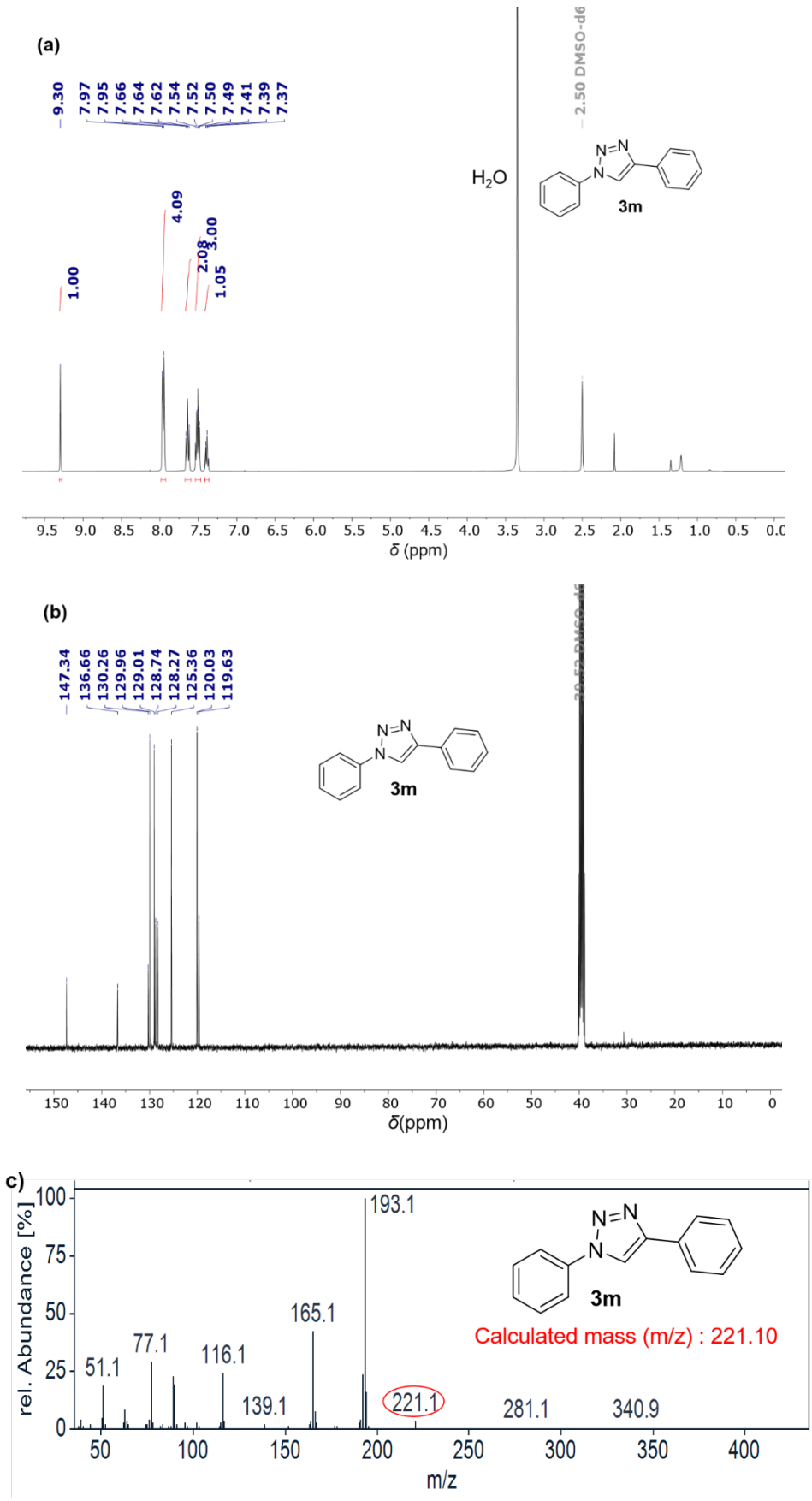

Fig. S23 (a) ^{1}H-NMR (400 MHz, DMSO-d_6, 298 K), (b) ^{13}C-NMR (100 MHz, DMSO-d_6, 298 K, (c) GC-MS spectra of **3m**.

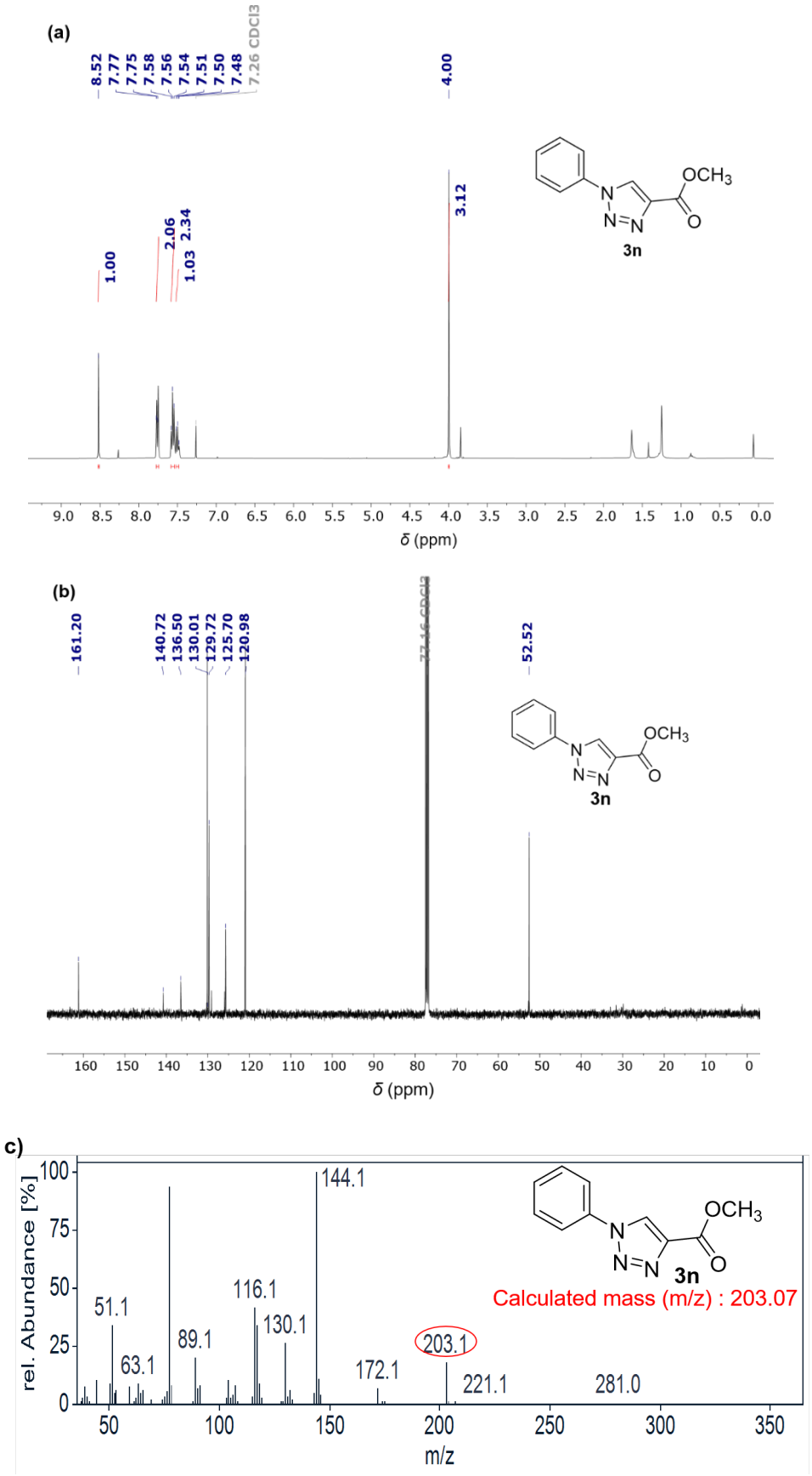

Fig. S24 (a) ^{1}H-NMR (400 MHz, $CDCl_3$, 298 K), (b) ^{13}C-NMR (100 MHz, $CDCl_3$, 298 K, (c) GC-MS spectra of **3n**.

Section E: References

S1 R. C. Mundargi, M. G. Potroz, J. H. Park, J. Seo, E. L. Tan, J. H. Lee and N. J. Cho, *Sci. Rep.,* 2016, **6**, 19960.

S2 A. Selim, K. M. Neethu, V. Gowri, S. Sartaliya, S. Kaur and G. Jayamurugan, *Asian J. Org. Chem.,* 2021, **10**, 3428–3433.

S3 K. D. Siebertz and C. P. Hackenberger, *Chem. Comm.,* 2018, **54**, 763–766.

S4 A. Xie, X. Xu, J. Li, B. Wang and W. Dong, *Asian J. Org. Chem.,* 2014, **3**, 1278–1283.

S5 S. Rohilla, S. S. Patel and N. Jain, *Eur. J. Org. Chem.,* 2016, **4**, 847–854.

S6 B. Mohan, H. Kang and K. H. Park, *Inorg. Chem. Commun.,* 2013, **35**, 239–241.

S7 Y. Chen, Z. J. Zhuo, D. M. Cui and C. Zhang, *J. Organomet. Chem.,* 2014, **749**, 215–218.

S8 L. Luciani, E. Goff, D. Lanari, S. Santoro and L. Vaccaro, *Green Chem.,* 2018, **20**,183–187.

S9 G. Chakraborti, R. Jana, T. Mandal, A. Datta and J. Dash, *Org. Chem. Front.,* 2021, **8**, 2434–2441.

S10 D. Drelinkiewicz and R. J. Whitby, *RSC Adv.,* 2022, **12**, 28910–28915.

S11 S. Borukhova, A. D. Seeger, T. Noël, Q. Wang, M. Busch and V. Hessel, *ChemSusChem,* 2015, **8**, 504–512.